ELSEVIER

Journal of Hazardous Materials 2261 (1999) xxx

Journal of Hazardous Materials

www.elsevier.nl/locate/jhazmat

Effects of aquifer heterogeneity and reaction mechanism uncertainty on a reactive barrier

Gerald R. Eykholt [*], Carl R. Elder [1], Craig H. Benson [2]

Department of Civil and Environmental Engineering, University of Wisconsin, Madison, WI, 53706, USA

Received 21 May 1998; revised 4 December 1998; accepted 10 December 1998

Abstract

This paper addresses impacts of aquifer heterogeneity and reaction mechanism uncertainty on permeable reactive barrier (PRB) performance and describes modeling tools and preliminary guidelines for risk-based design of reactive barriers at heterogeneous sites. A braided stream aquifer was generated stochastically, using a fixed correlation structure and four levels of variability in the hydraulic conductivity field. A vertical, homogeneous barrier was placed in the aquifer. Based on a deterministic design, the size of the PRB for uniform conditions was considered conservative (factor of safety = 3.3). Monte Carlo simulation was used to model *cis* 1,2-DCE reduction by iron metal with uncertainty in the reaction mechanism rate constants. These results were combined with flow and particle tracking results to predict the spatial distribution and flow-averaged concentrations of *cis* 1,2-DCE and vinyl chloride at the exit face of the PRB. Evaluated on a risk basis, the deterministic design method was found to be unconservative for more heterogeneous aquifers. Uncertainty in the reaction mechanism accentuated the negative effects of aquifer heterogeneity. Several compensating factors that may reduce the vulnerability of reactive barriers to aquifer heterogeneity are discussed.

Keywords: Reactive barrier; Uncertainty; Monte Carlo simulation; Reaction modeling; Aquifer heterogeneity; Groundwater flow modeling

[*] Corresponding author. Tel.: +1-608-263-3137; Fax: +1-608-262-5199; E-mail: eykholt@engr.wisc.edu
[1] E-mail: crelder@students.wisc.edu.
[2] E-mail: benson@engr.wisc.edu.

0304-3894/99/$ - see front matter
PII: S0304-3894(99)00032-1

1. Introduction

Reactive barriers serve as a containment technology. As contaminated groundwater flows off site, contaminants may be reduced by barrier media to concentrations below target values, which often are set at the maximum contaminant level (MCL) [1–4]. Groundwater velocity, barrier reactivity, and contaminant concentration among other factors affect the required size of a barrier. The groundwater velocity may be determined from hydrogeologic data and groundwater modeling, and the reactivity of the barrier media may be determined from laboratory and pilot column tests [5].

This paper presents an uncertainty-based technique for flow and reaction modeling of reactive barriers. The level of sophistication of existing models is adequate for preliminary design and assessment. However, often there is significant uncertainty in the parameters for the reaction mechanism and flow models. Also, the level of aquifer characterization and requirements of the design vary from site to site, and both spatial and temporal uncertainty exist in contaminant concentrations and barrier reactivity. The design problem amidst these uncertainties is difficult to solve, especially with existing models. However, the main question for many sites is the same: what level of quality assurance is obtained given the level of uncertainty and expected variability in hydrogeology and the reaction mechanism?

The goal of this paper is to discuss how spatial variability in aquifer hydraulic conductivity and uncertainty in the reaction mechanism rate constants can affect the performance of reactive barriers. This goal is met through flow and reaction rate modeling. Reactive barrier design also involves many other issues, such as optimal placement of the barrier, emplacement techniques, monitoring strategies, cost considerations, and aging issues [5]. Heterogeneity caused by these factors may lead to preferential flow and variable reactivity within the barrier. Although these factors are believed to affect barrier design, they are not included in this paper. The combined impact of heterogeneity in the aquifer and barrier is currently being studied by the authors and will likely be a topic for further research.

2. Background

2.1. Steady-state solutions, first-order transformations

van Genuchten [6] presented the steady-state solution for the ratio of effluent and influent concentrations, C_{ss} and C_{in}, respectively, with first-order degradation and one-dimensional flow as:

$$\frac{C_{ss}}{C_{in}} = \exp\left(\frac{(v-u)W}{2D}\right), \tag{1}$$

where v is the interstitial groundwater velocity (i.e., seepage velocity), W is the barrier

width (in the direction of flow), and D is the effective dispersion coefficient. The variable u is defined as:

$$u = v\sqrt{\frac{1+4kD}{v^2}}\,, \tag{2}$$

where k is the first-order rate constant. If dispersion is ignored, the plug-flow approximation is obtained:

$$\frac{C_{ss}}{C_{in}} \approx \exp\left(\frac{-kW}{v}\right). \tag{3}$$

For transport dominated by advection, the conversion predicted by the plug-flow approximation will coincide with that predicted when dispersion is considered [3].

The design task is to determine a barrier width (W) that achieves a targeted amount of conversion for the expected groundwater velocity and reaction rate constant. If plug-flow is assumed, the predicted barrier width (W_{PFR}) is:

$$W_{PFR} = -\frac{v}{k}\ln\left(\frac{C_{ss}}{C_{in}}\right). \tag{4}$$

For 1000-fold conversion, a reaction rate constant of 8.3/day (2.0 h half-life), and groundwater velocity of 0.50 m/day, W_{PFR} is 0.42 m, the design barrier width, W_d, is:

$$W_d = W_{PFR}\mathrm{CF_D}\mathrm{FS_W}, \tag{5}$$

where $\mathrm{FS_W}$ is the factor of safety for barrier width and $\mathrm{CF_D}$ is a dispersion correction factor [2]:

$$\mathrm{CF_D} = \left[\frac{\lambda}{\sqrt{1-2\lambda}-1}\right]. \tag{6}$$

The parameter λ is a nondimensional number equal to $2Dk/v^2$. The dispersion correction factor $\mathrm{CF_D}$ generally ranges from 1.0 (low dispersion) to 2.0 (high dispersion and high reaction rate constant).

Selecting the barrier width using Eqs. (1)–(6) assumes that flow and reaction rates are uniform temporally and spatially. This is uncommon in most aquifers. The factor of safety for barrier width accounts for uncertainty in the rate constant, groundwater velocity, and other design parameters. Contours of $\mathrm{FS_W}$, obtained via Monte Carlo simulation by Eykholt [7], are shown in Fig. 1. These factors of safety correspond to a 5% probability that effluent concentrations will exceed target concentrations. If W_{PFR} and $\mathrm{CF_D}$ are based on mean values for k, v, D, and C_{in}, $\mathrm{FS_W}$ range from 2.0 to 5.5 or higher [7]. However, it is unclear whether the $\mathrm{FS_W}$ reported by Eykholt [7] are appropriate for three-dimensional flow systems.

Required barrier widths for a wide range of chlorinated aliphatic compounds and $\mathrm{FS_W} = 1$ were presented by Tratnyek et al. [2]. Preliminary design curves for barrier

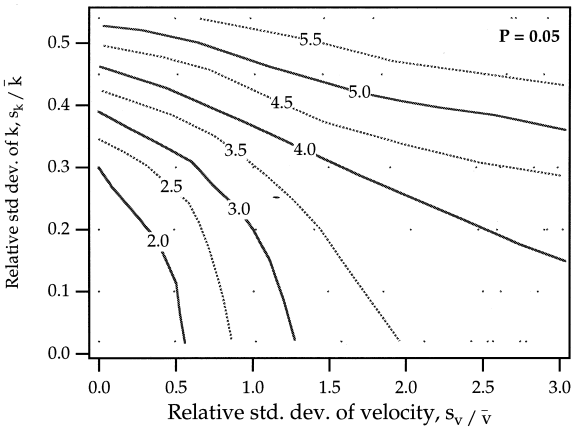

Fig. 1. Factors of safety for barrier width (FS_W) obtained from Monte Carlo simulation. Model assumes 1000-fold reduction in reactive barrier, 5% probability of failure that effluent concentration exceeds the target concentration, normal variation in rate constant, log-normal variation in the velocity, and log-normal variation in the input concentration with relative standard deviation of 10% [7].

width were based on best estimates of first-order rate constants normalized to iron surface area (k_{SA}). A convenient scaling relationship was also discussed:

$$W_{PFR} = \left(\frac{1.0 \dfrac{m^2}{ml}}{\rho_a} \right) \left(\frac{\log(C_{in}/C_{ss})}{3.0} \right) W_{ref}, \tag{7}$$

where W_{ref} is the reference width calculated using a specific surface area ρ_a of 1.0 m^2/ml and 1000-fold conversion. The design widths can be estimated using Eq. (5).

An important limitation of Eqs. (1)–(7) is that intermediate species are either ignored or assumed to be inconsequential. For instance, the production and depletion of vinyl chloride is not considered when evaluating the degradation of trichloroethylene (TCE), tetrachloroethylene (PCE), or dichloroethylene (DCE) isomers. In addition, the rate constants are not corrected for temperature, flow rate, aging, or other conditions that may vary between the laboratory and field [5,8].

2.2. First-order reaction networks

Roberts et al. [9] discussed a 10-member reaction network for the reductive dechlorination of chlorinated ethylenes by zero-valent metals. The proposed reaction mechanism is shown in Fig. 2. Although an irreversible first-order reaction network is assumed, a quantitative description of the complete network (e.g., rate constants, sorption parameters) has not yet been reported in the literature. Johnson et al. [10] have presented a summary of lumped rate constants for a variety of compounds, but little information has been presented on branching ratios that might describe preferential reaction pathways.

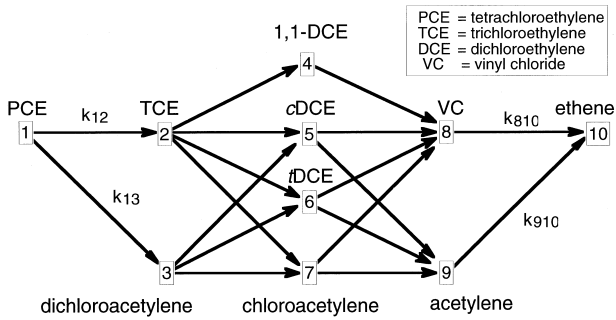

Fig. 2. Mechanism for reductive dechlorination and elimination of chlorinated ethene system proposed by Roberts et al. [9].

Higher-order and mixed-order kinetic models may be needed to characterize the reaction and sorption mechanism properly [11].

Eykholt [12] describes an analytical solution for networks of irreversible, first-order reactions. Assuming that initial concentrations are known and rate constants are fixed, the general solution follows the form of the characteristic solution:

$$C_j = \sum_i \boldsymbol{D}_{ij} e^{-\kappa_i t} \qquad (\text{for all values of } j), \tag{8}$$

where C_j is the concentration of 'daughter' product (or intermediate) species j affected by a combination of 'parent' or 'ancestor' species i, $\mathbf{D}_{ij}$ is a coefficient matrix, κ_i is a lumped, first-order rate constant, and t is time. Eykholt [12] provides examples and extensions of the method, including zero-order sources and instantaneous, reversible sorption. The general analytical solution for irreversible, first-order networks can be used for reactive barrier design if plug flow is assumed.

Tratnyek et al. [2] discuss simulation of a simplified reaction pathway for PCE to ethene (involving TCE, *cis* 1,2-DCE, VC, and acetylene). This analysis showed that conservative designs are obtained when the total molar concentration of chlorinated ethenes is assumed to be *cis* 1,2-DCE. No other combinations of species with the same total molar concentration yielded higher estimates for barrier width. Incidentally, the minimum barrier width was found when the total initial molar concentration was assumed to be vinyl chloride.

2.3. Aquifer heterogeneity

Natural aquifers are rarely homogeneous, yet this assumption is often made to simplify design and because data needed to characterize heterogeneity are unavailable [5]. One approach to characterize aquifer heterogeneity is to describe the spatial distribution of hydraulic conductivity by a probability density function for hydraulic conductivity at a point (usually log-normal) and an autocorrelation function [13]. The autocorrelation function is used to describe the spatial correlation structure of the aquifer. Stochastic simulation is used to generate random fields of hydraulic conductiv-

ity which can be input into a groundwater flow model. Another method used is multiple indicator geostatistics, where locations of facies are simulated first, and hydraulic conductivities are assigned to each facies [14,15]. In either method, realizations define a heterogeneous aquifer which can be modeled using conventional tools [5].

3. Methods

A five-step modeling approach was used in this study (Fig. 3). In Step 1, aquifers with heterogeneous hydraulic conductivity were generated. A homogeneous reactive barrier was placed in the center of each aquifer and the steady-state head solution was determined. In Step 2, fluxes entering and exiting the reactive barrier were calculated. Transit times for particles traveling through the reactive barrier were determined in Step 3. In Step 4, Monte Carlo simulation was used to estimate concentration distributions of *cis* 1,2-DCE and vinyl chloride as a function of residence time in the barrier. In Step 5, the results of Steps 2, 3 and 4 were combined to estimate concentrations of *cis* 1,2-DCE and vinyl chloride exiting the reactive barrier.

3.1. Groundwater flow modeling and particle tracking

The conceptual model for the flow modeling is a fully penetrating, reactive barrier 4.0 m long by 1.0 m wide, placed in the center of an 8.0 m wide by 8.0 m long by 2.8-m-thick section of an unconfined aquifer (Fig. 4). MODFLOW [16] was used to obtain the steady-state head solution. Transit times through the reactive barrier were estimated using PATH3D®, a particle tracking code [17]. The model has 14 layers, each with 1600 cubic cells 0.2 m wide. Constant head boundaries of 10.00 and 10.08 m were applied at the two ends, resulting in an average hydraulic gradient of 0.01-oriented perpendicular to the reactive barrier. Zero flux boundaries were applied along the other sides and bottom of the model (Fig. 4).

3.1.1. Aquifer simulation

The hydraulic conductivity distribution in each layer of the aquifer is a single realization generated using the Monte Carlo method. Hydraulic conductivity was assumed to follow a correlated, three-parameter log-normal (3PLN) random field. Realizations were generated by direct inversion of a correlated, multivariate normal matrix. Standard normal variates were generated by the Box–Mueller method, and Cholesky decomposition was used for the inversion.

The 3PLN distribution was selected because it provides a good fit to hydraulic conductivity data for a braided stream deposit described by Webb and Anderson [18] and Aiken [19]. Probability density functions (PDFs) describing the hydraulic conductivity fields in this study are shown in Fig. 5.

The log-mean hydraulic conductivity ($\mu_{\ln K}$) was -10.3, which corresponds to 8.4×10^{-5} m/s. This equals the geometric mean hydraulic conductivity for the braided stream deposit reported by Webb [20], Aiken [19] and Riemersma [21]. The log-standard deviation of hydraulic conductivity ($\sigma_{\ln K}$) was assigned values of 0.5 (nearly homoge-

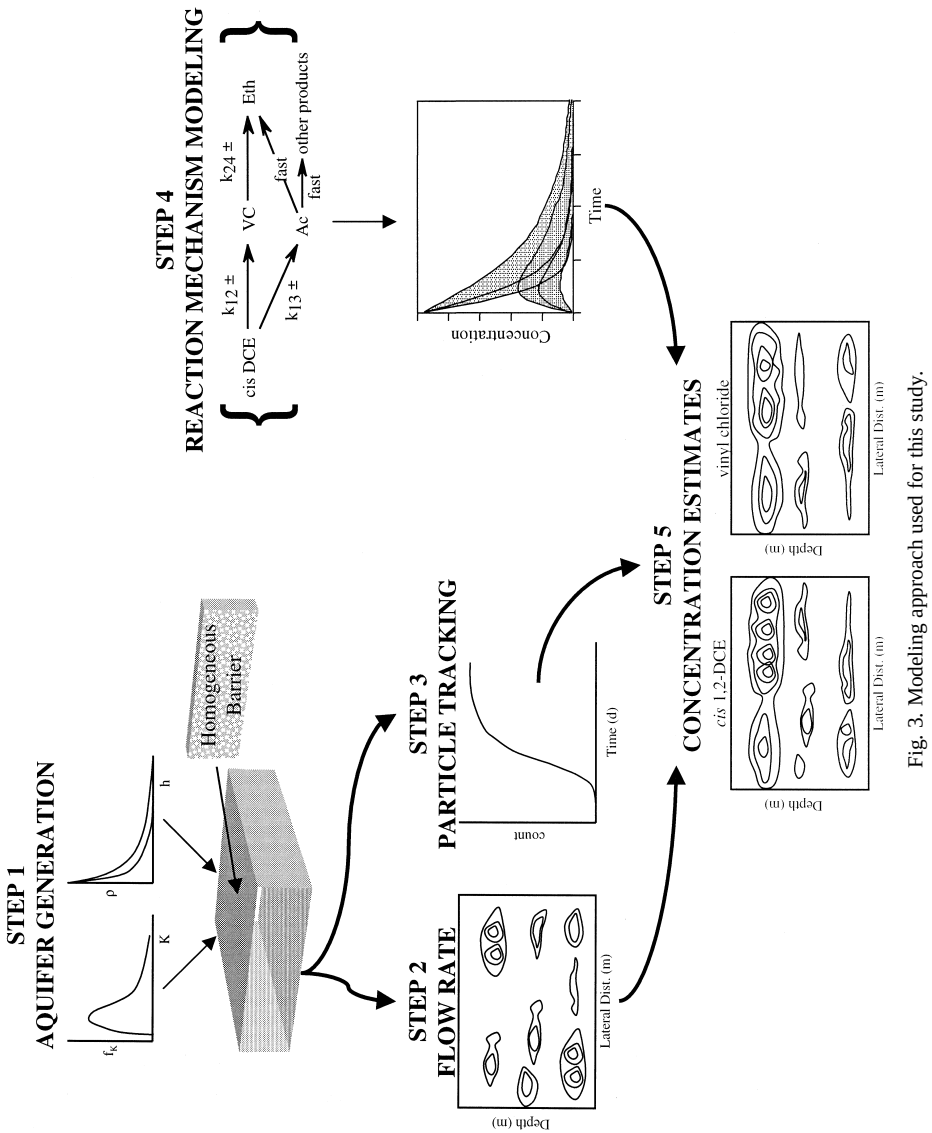

Fig. 3. Modeling approach used for this study.

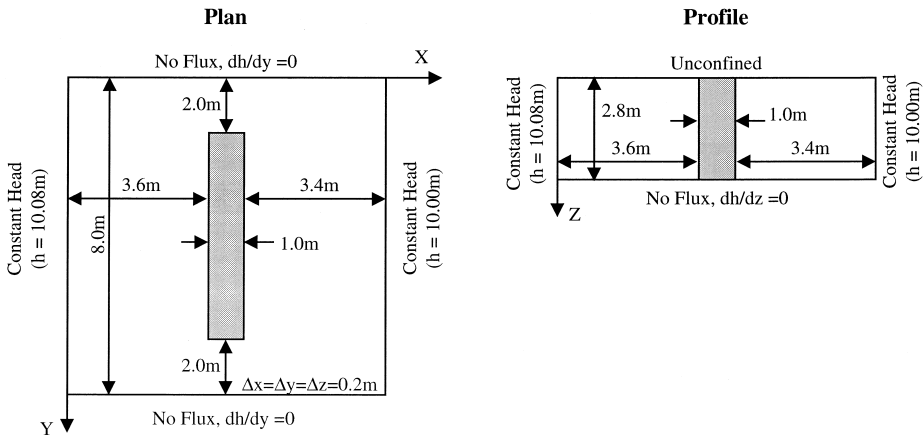

Fig. 4. Conceptual model for flow modeling and particle tracking.

neous aquifer), 1.0, 1.5, and 2 (moderately heterogeneous aquifer). Riemersma [21] reports that braided stream deposits have $\sigma_{\ln K}$ between 1.2 and 3.3. Jussell et al. [22,23] measured a geometric mean hydraulic conductivity of 1×10^{-4} m/s for heterogeneous sandy gravel aquifers and $\sigma_{\ln K}$ of 1.8.

Analysis of data obtained from dense sampling and excavation mapping of coarse-grained, alluvial deposits indicate that correlation lengths in the longitudinal and lateral directions (λ_x and λ_y) vary from 5 m [22,23] to 40 m [20]. In this study, correlation in the horizontal plane was simulated using an exponential correlation function with λ_x and λ_y of 6 and 3 m, respectively (Fig. 6). Correlation length in the vertical direction (λ_z) is typically less than 0.5 m [22,23,20]. Since the correlation length in the vertical

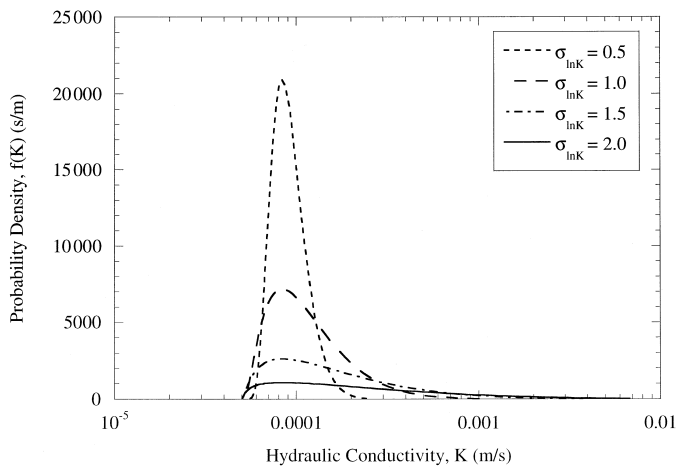

Fig. 5. Correlation structure used for generating hydraulic conductivity fields.

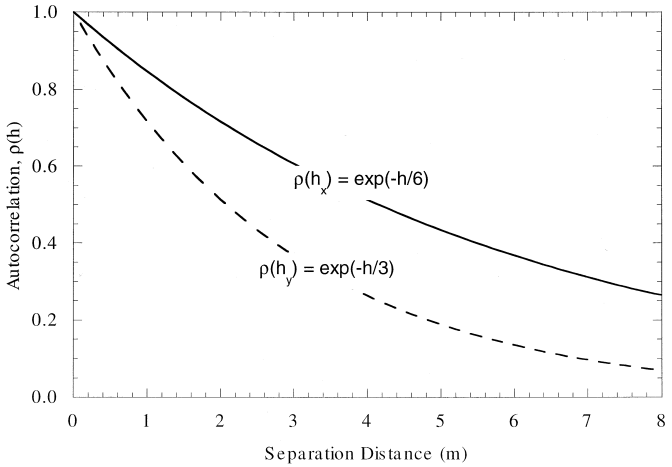

Fig. 6. Probability density functions for the hydraulic conductivity fields.

direction is close to the grid spacing used for the model, hydraulic conductivities between the layers were uncorrelated.

A homogeneous reactive barrier was incorporated into the random field by replacing the hydraulic conductivities in the central region of the aquifer with a constant hydraulic conductivity of 0.0025 m/s (Fig. 4). This is the geometric mean hydraulic conductivity obtained from 40 laboratory measurements on mixtures of well-graded sand and coarse iron filings (Peerless Metal Powders, +8–50 mesh). Results of these tests showed that the hydraulic conductivity of sand/iron mixtures is approximately normally distributed with a measured coefficient of variation of 0.31. Thus, the assumption of a constant hydraulic conductivity for the reactive barrier is reasonable.

The same sequence of uniform random numbers and correlation structure was used for all realizations, yielding similar spatial patterns of hydraulic conductivity. This technique was selected to distinguish differences in flow and travel time from variations arising from dependent realizations (i.e., changing $\sigma_{\ln K}$). Thus, the simulated aquifers can be viewed as having different levels of variability, but structural similarity.

3.1.2. Particle tracking and residence times

The particle tracking code PATH3D® was used to calculate travel times for 280 particles that passed through the reactive barrier. Particles were placed on a 0.2 m grid along the up-gradient face of the barrier and tracked until they reached the downstream (10.00 m) constant head boundary. The time and position of the particles exiting the barrier were reported and used for calculating the extent of chemical reduction occurring in the barrier. For all simulations, the product of porosity and retardation factor was assumed equal to 0.5. This is representative of an aquifer with a porosity of 0.35 and retardation of 1.4. In addition, the flow rate entering and exiting the barrier was calculated for each grid element using the heads in adjacent cells. Flow rates were used to assign a mass to each particle entering the barrier.

3.2. Reaction mechanism modeling

There is considerable uncertainty in reaction rate constants and preferential pathways for the reduction of chlorinated ethenes by iron metal. However, as discussed previously, a conservative analysis can be obtained if the total molar concentration for chlorinated ethenes is *cis* 1,2-DCE [2]. A simplified reaction network for the reduction of *cis* 1,2-DCE and the intermediate product of vinyl chloride is shown in Fig. 7. The rate constants are consistent with lumped, first-order decay rate constants for *cis* 1,2-DCE ($\kappa_{1,SA} = 4.1 \pm 1.7 \times 10^{-5}$ l/m^2 h) and vinyl chloride ($\kappa_{1,SA} = 5.0 \pm 1.5 \times 10^{-5}$ l/m^2 h) as reported by Johnson et al. [10], a specific surface area (ρ_a) of 3.5 m^2/ml, and a branching ratio of 0.70 for the formation of vinyl chloride. While levels of vinyl chloride predicted from this simulated reaction network are generally 50% higher than levels observed in laboratory experiments [24,25], other factors, such as incomplete carbon balances and reaction orders other than one, warrant conservative predictions for vinyl chloride formation. Assumptions regarding vinyl chloride formation are a critical part of the analysis, since vinyl chloride has a low target concentration (MCL = 2.0 μg/l) compared to *cis* 1,2-DCE (70 μg/l).

Normal distributions were assumed for first-order rate constants in the network. A constant input concentration of 10 μM (970 μg/l) of *cis* 1,2-DCE was assumed, and the initial vinyl chloride concentration was assumed to be zero. Monte Carlo simulation of the reaction network was based on the prior work of Eykholt [7]. For fifty times ranging from 0 to 5.0 days, 1000 uncorrelated realizations were generated for each network rate constant for a target mean and standard deviation. A non-negativity constraint was placed on first-order rate constants. Molar concentrations of each network species were determined using the analytical solution (Eq. (8)Eqs. 9–11).

Concentrations corresponding to the 0.05, 0.25, 0.50, 0.75, and 0.95 percentiles were reported and the mean, standard deviation, skew, and kurtosis were determined. The concentration distributions had high negative skew (concentrations fell below the mean). Simulated concentrations of *cis* 1,2-DCE and vinyl chloride corresponding to the probability levels of 0.05, 0.50, and 0.95 were plotted vs. time.

Results of the Monte Carlo simulations of the reaction mechanism were combined with particle residence times, t_i, from the flow model to determine the concentration of each particle at the exit face. Concentrations corresponding to the 0.05, 0.50, and 0.95 percentiles of the reaction mechanism were reported.

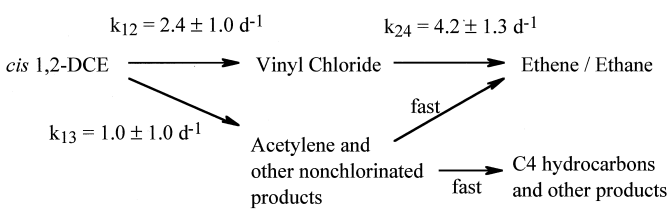

Fig. 7. Simplified reaction network for the reduction of *cis* 1,2-DCE and vinyl chloride.

3.3. Concentrations at the exit face of the reactive barrier

Although particles were introduced at the up-gradient face of the reactive barrier with uniform spacing, the particle trajectories were irregular, and two or more particles were found to exit the barrier through the same cell in the finite difference grid. As each particle was tracked, information was gathered regarding the input location, transit time t_i, input flow rate in the longitudinal direction Q_i, and exit face output coordinates (Y_j, Z_j). The flow-averaged concentration on the exit face C_j was estimated as:

$$C_j = \frac{\sum_i Q_i C_i \mathbf{U}_{ij}}{\sum_i Q_i \mathbf{U}_{ij}}, \tag{12}$$

where j is the position index on the exit face and i is the position index at the input face. Elements of the matrix $\mathbf{U}_{ij}$ are equal to one for the particle that enter the barrier at position index i and exit from position j, but are equal to zero otherwise. Although the particle may exit at the irregularly spaced face coordinates (Y_j, Z_j), the particle reports to a particular exit face node region ($Yn_j \pm 0.1$ m, $Zn_j \pm 0.1$ m). The effluent concentration of each particle C_i is determined from Eq. (12). Contours were generated with 16 times interpolation using IgorPro 3.1 (WaveMetrics).

With the assumption of complete mixing of particles downstream of the barrier, flow-averaged concentrations for *cis* 1,2-DCE and vinyl chloride were calculated:

$$\bar{C} = \frac{\Sigma Q_i C_i}{\Sigma Q_i}. \tag{13}$$

Flow-averaged concentrations for *cis* 1,2-DCE and vinyl chloride were calculated and plotted for three reaction mechanism probability levels (0.05, 0.50, and 0.95) and for the four cases of $\sigma_{\ln K}$.

4. Results and discussion

4.1. Deterministic design

A deterministic design width for the scenario under consideration in this study was made using average parameters for the aquifer and reaction mechanisms (Eq. (4)) and a factor of safety. Comparisons with this estimate will be made throughout the paper. Given an average gradient of 0.01, hydraulic conductivity of 8.4×10^{-5} m/s, and barrier porosity of 0.50, the average seepage velocity is 0.15 m/day. Using the analytical solution (Eq. (8)Eqs. 9–11) and an initial concentration of 10 μM of *cis* 1,2-DCE, a residence time of 2 days is required for reduction of vinyl chloride to below the MCL (2 μg/l). For these conditions, a barrier design width of 1.0 m provides a residence time of 6.6 days and a factor of safety (FS_W) of 3.3.

4.2. Groundwater flow modeling

4.2.1. Aquifer heterogeneity

The hydraulic conductivity fields for two simulated aquifers in layer 7 ($Z = 1.2$ to 1.4 m) are shown in Fig. 8. As mentioned above, the aquifers were generated using the same random number sequence and correlation structure, so the two cases differ primarily in $\sigma_{\ln K}$ (1.0 vs. 2.0). The contrast between the hydraulic conductivity of the reactive barrier and surrounding soils is evident in Fig. 8. The reactive barrier has a uniform hydraulic conductivity of 2.5×10^{-3} m/s which is higher than the hydraulic conductivity in most of the aquifer. Also, the transition between the hydraulic conductivity of the aquifer and reactive barrier is more abrupt than the transitions between regions of high and low hydraulic conductivity within the aquifer.

4.2.2. Flow exiting the reactive barrier

Flow rates from the reactive barrier into the aquifer are shown in Fig. 9. When $\sigma_{\ln K} = 0.5$ (Fig. 9a), flow rate exiting the reactive barrier is uniform, with small regions of higher flow along the edges. These regions form because there is less resistance along the longer flow paths that transect the barrier. Particle tracking showed that water entering these regions has a higher velocity than in the surrounding aquifer. Therefore, even under nearly homogeneous conditions, preferential flow through the edges of the reactive barrier occurs.

For larger $\sigma_{\ln K}$, higher flow rates continue to occur along the edges of the reactive barrier, and additional regions of higher flow rate develop throughout the barrier. These regions tend to be short and wide, similar to the spatial structure incorporated into the hydraulic conductivity field for the aquifer. In aquifers where $\sigma_{\ln K} = 2$ (Fig. 9d), flow rate exiting the barrier may be 10 times greater than when $\sigma_{\ln K} = 0.5$. Also, when $\sigma_{\ln K} = 2.0$, flow rate throughout the barrier may vary by an order of magnitude.

High discharge rates from the reactive barrier correspond to regions of high hydraulic conductivity in the aquifer down-gradient of the reactive barrier. Thus, flow rate and residence time of particles in the barrier are strongly affected by the hydraulic conductivity of the aquifer down gradient of the barrier. Reactive barriers do not necessarily diffuse flow, and flow rate exiting reactive barriers is not uniform. Reactive barriers, however, may serve as a distributor of flow, connecting high conductivity regions that would otherwise not be connected. Thus, pea-gravel zones installed up-gradient of reactive barriers may not be as effective as believed, and more study is needed to assess their effectiveness.

When $\sigma_{\ln K}$ increases, regions of higher flow rate develop, but regions of lower flow rate do not. This is a consequence of the skewed distribution of the hydraulic conductivity of the aquifer (Fig. 5). For higher $\sigma_{\ln K}$, the upper tail of the PDF becomes heavier, increasing the probability of higher hydraulic conductivity. Also, the probability mass associated with lower hydraulic conductivities becomes smaller as $\sigma_{\ln K}$ increases, so few regions of lower flow rate develop.

4.2.3. Particle tracking

The trajectories of particles as they pass from the up-gradient face of the reactive barrier to the down-gradient boundary of the problem domain ($X = 3.6$ to 8 m, Fig. 4)

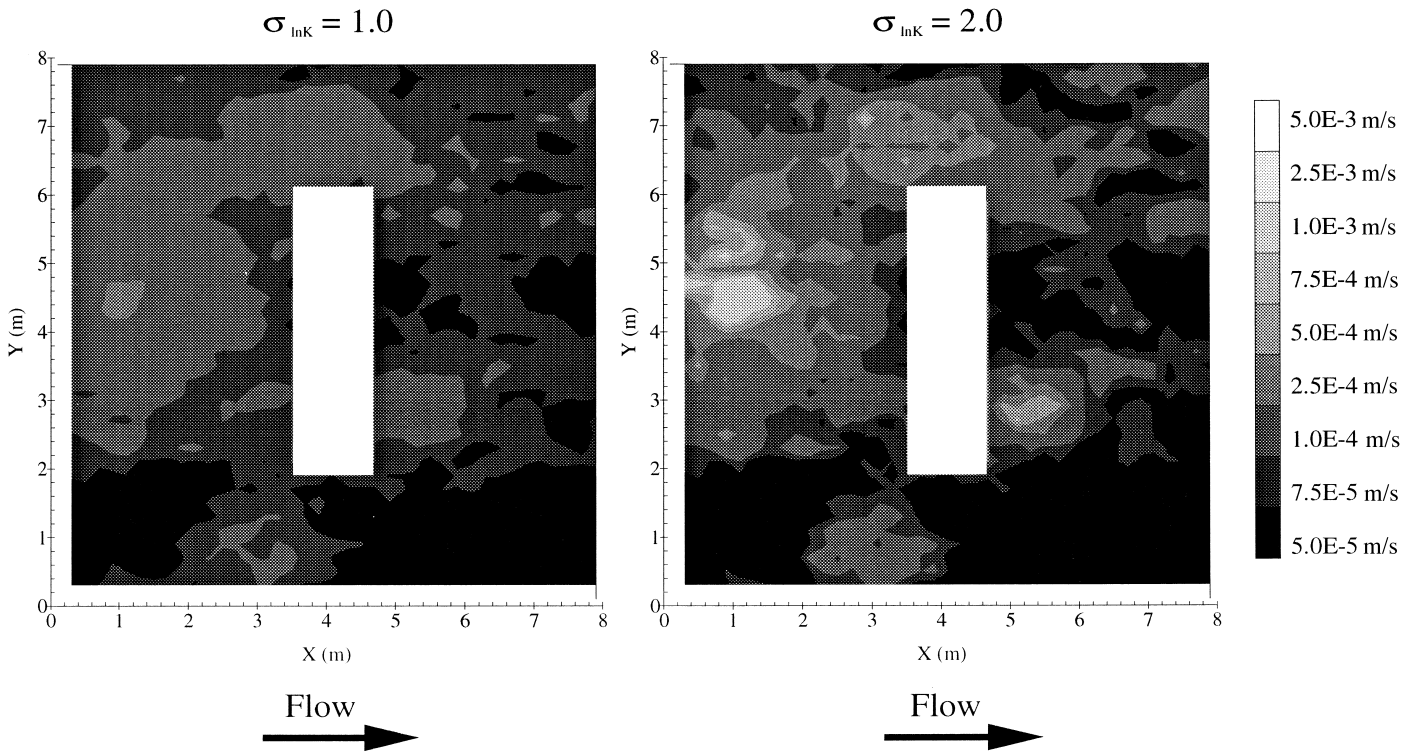

Fig. 8. Spatial distribution of hydraulic conductivity for two realizations of an aquifer at different $\sigma_{\ln K}$ using identical random number sequences.

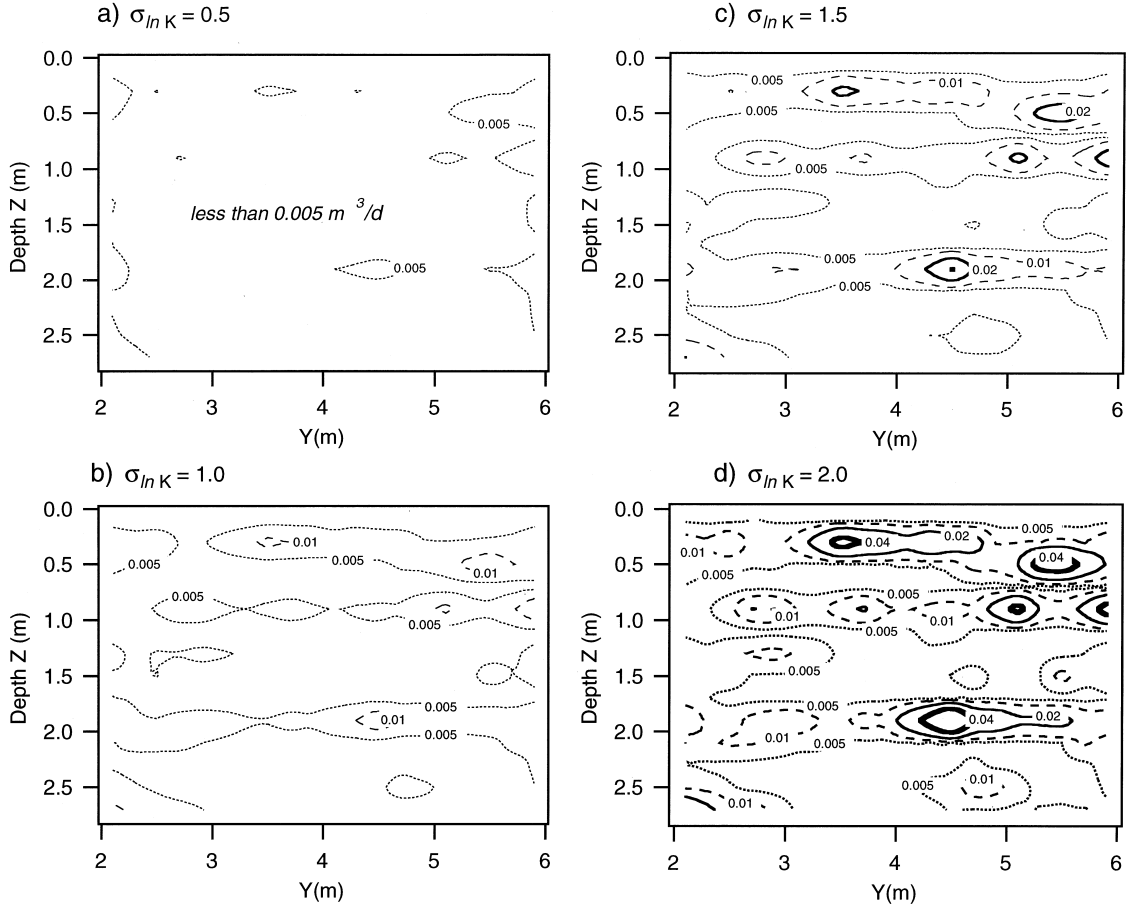

Fig. 9. Flow contours at the effluent face of a reactive barrier. ($Q = \mathrm{m}^3/\mathrm{day}$).

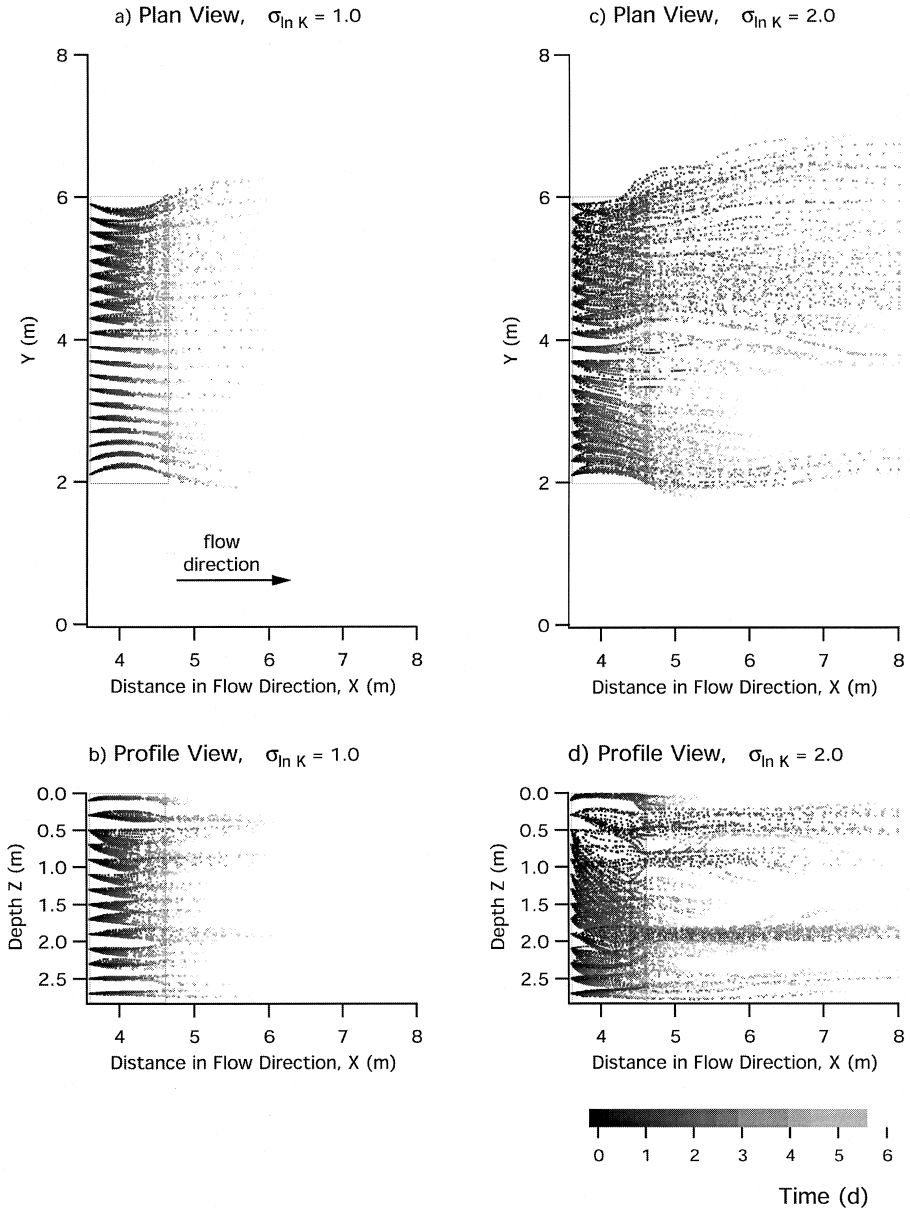

Fig. 10. Particle trajectory through reactive barriers.

are shown in Fig. 10 for simulations where $\sigma_{\ln K} = 1$ and 2. The symbols used in Fig. 10 decrease in size for particles located deeper in the wall, while colors from red to violet

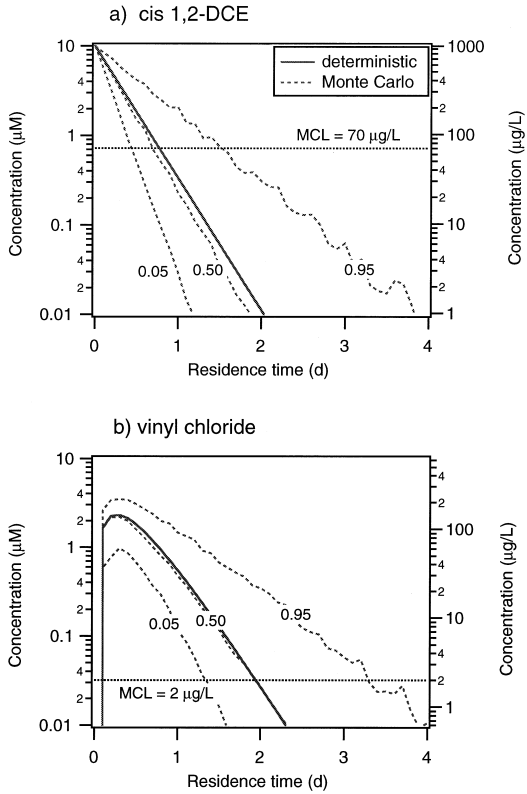

Fig. 11. Effects of uncertainty in rate constants on the reduction of *cis* 1,2 DCE and vinyl chloride by iron metal. Cumulative probability levels of 0.05, 0.50, and 0.95 as determined by 1000 Monte Carlo trials for each time are shown.

indicate time. Particle path lines through the reactive barrier and aquifer do not directly reflect the quantity of flow.

4.2.3.1. Aquifer with low heterogeneity ($\sigma_{\ln K} = 1$). When aquifer heterogeneity is low, particles travel through the reactive barrier in nearly straight path lines that are aligned parallel to the regional gradient of the aquifer. The median residence time for particles in the barrier is 4.6 days compared to 6.6 days for the homogeneous case (deterministic design). There is a slight curvature of path lines near the edges of the reactive barrier ($Y = 2$ and 6 m), indicating a slightly higher gradient in these regions than in the rest of the reactive barrier. Consequently, travel times are slightly shorter in these areas. Once

Fig. 12. Contours of vinyl chloride concentration (μg/l) on exit face of reactive barrier in simulated aquifer: effect of $\sigma_{\ln K}$. Concentrations represent median case (0.50) for Monte Carlo simulations on reaction mechanism and input *cis* 1,2 DCE concentration of 10 μM (970 μg/l).

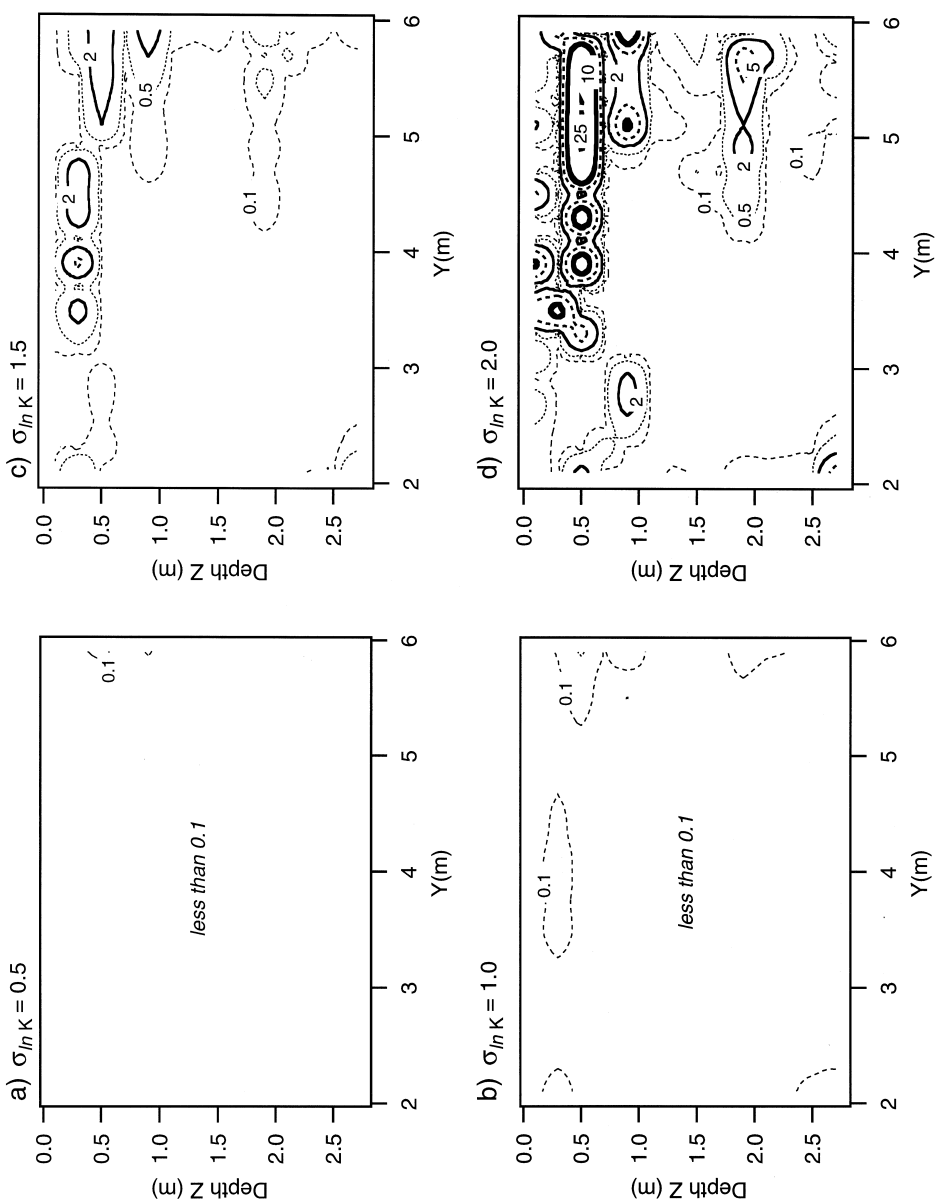
a) σln K = 0.5
b) σln K = 1.0
c) σln K = 1.5
d) σln K = 2.0
Depth Z (m)
Y(m)
less than 0.1
0.1
0.5
2
5
10
25

particles exit the barrier and enter the aquifer, they disperse into a plume that is wider than the reactive barrier. There is little funneling of flow or mixing observed within the barrier except in the profile view.

In the profile view, flow is horizontal and travel times are uniformly distributed. The only observable preferential flows for the $\sigma_{\ln K} = 1$ case occur at depths of 0.25, 0.75, and 1.75 m. These may be caused by regions of higher hydraulic conductivity down-gradient of the barrier. Travel times of particles after they exit the barrier are affected more than travel times within the barrier.

4.2.3.2. Aquifer with high heterogeneity ($\sigma_{lnK} = 2$). In general, travel times are shorter for particles passing through a reactive barrier when $\sigma_{\ln K} = 2$. For example, the median residence time for particles in the barrier is 2.9 days when $\sigma_{\ln K} = 2$, compared to 6.6 days for the homogeneous case and 4.6 days when $\sigma_{\ln K} = 1$. As a result, overall contaminant degradation is less per unit width of reactive barrier as the heterogeneity of the aquifer increases, even when the geometric mean hydraulic conductivity of the aquifer is unchanged. The path lines when $\sigma_{\ln K} = 2$ are more curved, and there appears to be more mixing within the barrier. In contrast to $\sigma_{\ln K} = 1$, path lines through a reactive barrier in an aquifer with $\sigma_{\ln K} = 2$ are oriented away from the center of the reactive barrier (plan view). This results in less curvature of path lines near the edge of the barrier because there is a greater component of lateral flow. The additional lateral flow also causes particles to exit the edge of the barrier, which did not occur in the simulation when $\sigma_{\ln K} = 1$. Particles exiting the edge of the barrier may represent a source for intermediate products of the reduction process since these particles have a shorter residence time in the barrier.

The impact of aquifer heterogeneity on particle travel times is most noticeable in the profile views in Fig. 10. As particles pass through a reactive barrier when $\sigma_{\ln K} = 2$, they change elevation significantly, creating zones where no particles pass and zones of high particle density. This results in longer travel distances, but shorter travel times and higher particle velocities. Thus, longer travel distances (i.e., wider barriers) do not necessarily correspond to longer residence time in the barrier. Additionally, focused flow within the barrier may lead to more complex processes that are difficult to assess from batch or column laboratory experiments.

Two preferential flow paths at depths of 0.5 and 1.75 m are shown in the profile view when $\sigma_{\ln K} = 2$ (Fig. 10). Travel times for the particles exiting the barrier at these locations are one-fifth of travel times for particles in other parts of the barrier. These zones correspond to zones of higher hydraulic conductivity down-gradient of the barrier, since particles continue to travel quickly at these elevations after reentering the aquifer. The location of high hydraulic conductivity facies down-gradient of the barrier clearly influences flow through the barrier.

Particle trajectories within the reactive barrier are more tortuous in the vertical direction than in the lateral direction. Path lines in a homogeneous region form along the shortest path connecting zones of high hydraulic conductivity at the boundaries. Since the vertical correlation length in the aquifer is less than the lateral correlation length, regions of high hydraulic conductivity tend to be oriented in thin, elongated layers. Path lines within the homogeneous barrier tend to change elevation to connect these regions,

and more variability of flow with depth is expected. This effect is accentuated at $\sigma_{\ln K} = 2.0$, but is evident at $\sigma_{\ln K} = 1.0$ as well.

4.3. Reaction mechanism modeling

The effect of uncertainty in the reaction mechanism of *cis* 1,2-DCE and vinyl chloride reduction by iron metal, estimated from Monte Carlo simulation, is shown in Fig. 11 in terms of the 0.05, 0.50, and 0.95 concentration percentiles (P). The median case ($P = 0.50$) corresponds closely with the case determined from mean reaction rate (deterministic case). For times greater than 0.5 day, the median molar concentration of vinyl chloride is higher than the concentration of *cis* 1,2-DCE, but the two concentrations are within an order of magnitude of each other. Since the MCL of vinyl chloride is significantly lower than the MCL for *cis* 1,2-DCE, the reactive barrier design would most likely be dominated by the estimates for vinyl chloride concentration. Retention times required for vinyl chloride are 2.0 and 3.2 days for the 0.50 and 0.95 percentiles, respectively. Retention times required for *cis* 1,2-DCE are less than 2.0 days. If the design is based on mean rate constants and no uncertainty in the reaction mechanism, a factor of safety on barrier width (FS_W) less than 1.5 would compensate for the uncertainty in the reaction mechanism with a 95% probability of success.

4.4. Combined effects of aquifer heterogeneity and reaction mechanism uncertainty

The effect of aquifer heterogeneity (i.e., $\sigma_{\ln K}$) on reactive barrier performance is shown in Fig. 12. Vinyl chloride concentrations were determined using the median behavior of the reaction mechanism shown in Fig. 11 and the residence times obtained from the particle tracking code. For $\sigma_{\ln K} \leq 1.0$, the vinyl chloride concentrations are generally more than an order of magnitude below the MCL (2 μg/l). As $\sigma_{\ln K}$ increases to 1.5, approximately 10% of the exit face area has concentrations above the MCL and the peak concentration is above 5 μg/l. As $\sigma_{\ln K}$ increases to 2.0, approximately 20% of the exit face area has concentrations above the MCL and the peak vinyl chloride concentration is above 25 μg/l.

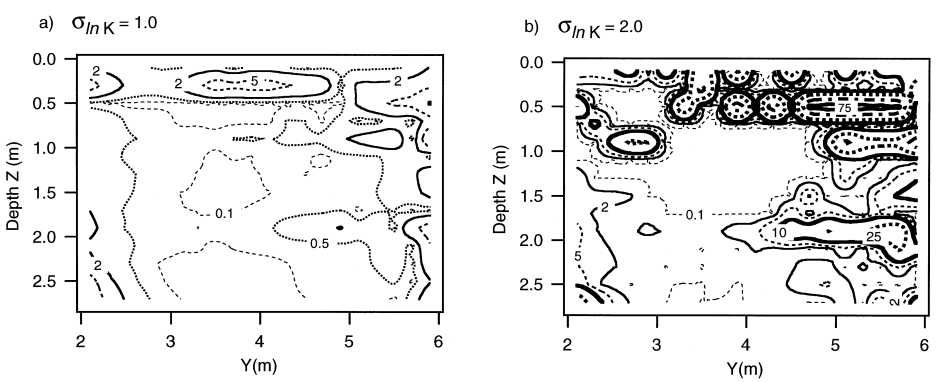

Fig. 13. Contours of vinyl chloride concentration (μg/l) on exit face of reactive barrier in simulated aquifer. Concentrations represent 0.95 cumulative probability level obtained from Monte Carlo simulations on reaction mechanism.

Regions of high exit face concentration do not necessarily correspond to regions of high flow (Figs. 10 and 12), especially for higher $\sigma_{\ln K}$ due to irregular particle trajectories within the barrier. A particle associated with a high effluent flow rate may take a tortuous path through the barrier and have a longer residence time. This may cause effluent concentrations to be lower than would be predicted had the trajectory been straight.

The combined effect of uncertainty in the reaction mechanism and spatial variability is shown in Fig. 13. Contours for the 0.95 percentile of vinyl chloride concentration are presented for two cases of $\sigma_{\ln K}$. The same general effects are shown; as $\sigma_{\ln K}$ increases, the concentration of vinyl chloride at the exit face increases significantly. However, the added effect of uncertainty in the reaction mechanism accentuates the problem. Vinyl chloride concentrations are above the MCL for a greater percentage of the exit face area, and peak concentrations are much higher. For instance, when $\sigma_{\ln K} = 1.0$, exit face concentrations exceed the MCL for vinyl chloride in a number of regions, whereas concentrations were at least an order of magnitude below the MCL when reaction rate uncertainty was not considered. In addition, when $\sigma_{\ln K} = 2.0$ more than 50% of the exit face area exhibits vinyl chloride concentrations above the MCL and the peak concentration is approximately 40 times the MCL.

There are several compensating factors that may dampen extremes in exit face concentration. The most important compensating factor is the use of hydrogeologic measurements (i.e., heads, pumping tests, tracer tests) within the site to determine the best placement of the barrier and better estimates of the design groundwater velocity. The deterministic design modeled in this paper was based on fixed heads at the site boundaries and the geometric mean hydraulic conductivity; more extensive hydrogeologic characterization would likely result in a more reliable design.

A negative correlation between flow rate and input concentration will dampen the negative effect of relatively fast particles. Facies with high hydraulic conductivity may be correlated with lower input concentrations. Higher flow rates within the reactive

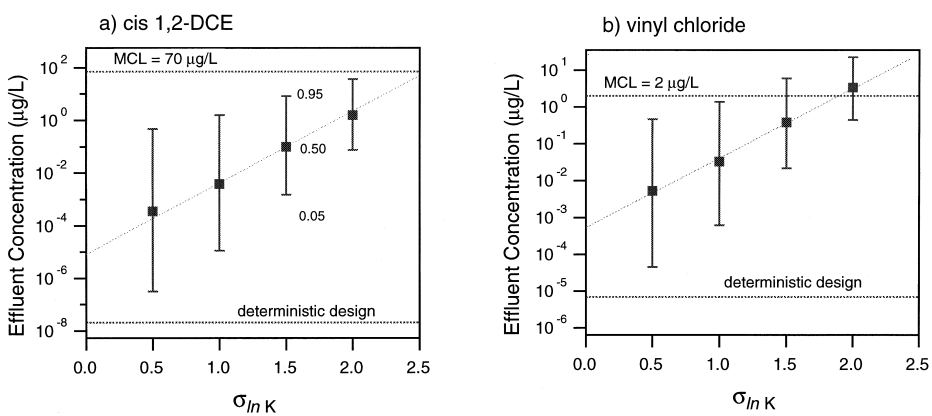

Fig. 14. Flow-averaged concentrations for exit face of barrier and for 0.05, 0.50, and 0.95 cumulative probability levels determined from Monte Carlo simulation on reaction mechanism.

barrier may also be correlated with higher reaction rate constants. Eykholt [7] demonstrated the compensating effect of parameter correlation on reactive barrier width. Multiple Monte Carlo simulations for uniform flow and first-order conversion in reactive barriers were performed. Positive correlation ($\rho = 0.7$) between the log-normal velocity and normally distributed rate constant resulted in a decrease in FS_W of 25% from the uncorrelated case at the 0.95 percentile and for a 30% coefficient of variation of the rate constant. The effects would be more significant for more uncertainty in the reaction mechanism and more heterogeneous flow through the barrier.

Another compensating effect is mixing downstream of the reactive barrier. Fig. 14 shows the 0.05, 0.50, and 0.95 percentiles of flow averaged concentration of *cis* 1,2 DCE and vinyl chloride at the exit face of barrier computed with Eq. (13). Several key points are evident. First, flow-averaged concentrations increase in a log-linear fashion with $\sigma_{\ln K}$. Second, the MCL for vinyl chloride is exceeded for $\sigma_{\ln K} > 1.0$ at the 0.95 percentile for the reaction mechanism, and for $\sigma_{\ln K} = 2.0$ at the 0.50 percentile for the reaction mechanism. For $\sigma_{\ln K} \leq 1.0$, the deterministic barrier design with $FS_W = 3.3$ may be considered safe, but not conservative. From this analysis, the deterministic design with $FS_W = 3.3$ is only adequate for aquifers with $\sigma_{\ln K} \leq 1.0$. For cases in which the uncertainty in the reaction mechanism is greater, or $\sigma_{\ln K} > 1.0$, $FS_W = 3.3$ may not be adequate.

As $\sigma_{\ln K}$ increases, the relative significance of uncertainty in the reaction mechanism is less important. However, for the cases considered here, neither uncertainty in the reaction mechanism nor heterogeneity in flow should be ignored. Both of these sources of uncertainty can be incorporated into design and analysis using existing tools as illustrated in this paper.

The criterion for a safe barrier width is unclear and arbitrary at this stage. In this analysis, a barrier design was considered acceptable if the flow-average concentration at the 0.95 percentile was below the MCL. Given this criteria, deterministic designs with $FS_W = 3.3$ were unacceptable for more variable aquifers. However, the MCL has been established with conservative assumptions regarding exposure and potency. A more elaborate, risk assessment method would incorporate exposure probabilities from the uncertainty-based design rather than enforcing a maximum exit concentration.

Other factors not considered by this analysis may further complicate barrier design. For instance, physical heterogeneity within the barrier resulting from construction or from placing the monitoring network can lead to a decrease in barrier reliability. Other factors that may change the degree of heterogeneity and reactivity near the barrier over long periods include colloidal transport, barrier clogging, microbiological activity, reactive barrier dissolution, and gas evolution. Several of these are currently being studied.

5. Conclusion

Reactive barrier performance is a function of spatial variability of the hydrogeologic properties of the aquifer and uncertainty in the reaction mechanism. Although other factors are important for barrier design, one of the most important issues is sizing the barrier to establish ample residence time of contaminants, such that contaminants and

any toxic intermediates are reduced to safe levels. Several sizing relationships for uniform flow conditions have been reviewed in this paper. However, the combined impact of spatial variability in flow and reaction mechanism uncertainty can be significant. This paper shows that a deterministic design based on uniform flow and average reactions rates can be unconservative for more variable aquifers ($\sigma_{\ln K} > 1.0$), despite a factor of safety of 3.3 on barrier width.

Uncertainty in the reaction mechanism has been shown to significantly affect effluent concentrations. For instance, the spatially-averaged vinyl chloride effluent concentrations at the 0.95 and 0.50 mechanism percentiles vary approximately 10,000% for low $\sigma_{\ln K}$ and approximately 1000% for moderate variability in hydraulic conductivity ($\sigma_{\ln K} = 1.5$). Furthermore, peak vinyl chloride concentrations at the exit face of the barrier for $\sigma_{\ln K} = 2.0$ are more than 10 times the MCL for the 0.95 reaction mechanism percentile and 40 times the MCL for the 0.50 reaction mechanism percentile. Other factors influencing the reaction mechanism, especially the order of the reactions and role of sorption, should be considered too.

Although there may be several compensating effects that dampen the extremes in exit face concentration and the design considerations at each site vary, some preliminary guidelines for sizing reactive barriers are evident.

(i) Site hydrogeology should be characterized with sufficient detail to describe the spatial distribution of hydraulic conductivity. Ideally, higher hydraulic conductivity facies should be mapped, as these facies will control flow rate and exit concentrations.

(ii) Quantitative information about branching to critical intermediate species, such as vinyl chloride should be defined when characterizing the reaction mechanisms. Not only should lumped rate constants be determined, but also specific mechanism rate constants and uncertainty information regarding mechanism parameter estimates should be gathered. Although rates and mechanisms may vary with iron selection and site groundwater conditions, more general information regarding mechanism characterization can reduce the effort required for each site.

(iii) The tools of Monte Carlo simulation of first-order reaction networks, flow modeling, and particle tracking are available. Once characterization data have been gathered, these tools can used to simulate ranges in expected performance of reactive barrier designs for particular sites. In addition, flow and concentration data gathered from recent installations can be analyzed to validate and calibrate the modeling used.

The main conclusions of this study address the impacts of aquifer heterogeneity and reaction mechanism uncertainty on reliability of a deterministic barrier design. The use of the same general tools to develop a more comprehensive, risk-based design method warrants further study.

Acknowledgements

Financial support for this study was provided by a National Science Foundation Career Award to Gerald R. Eykholt (Award No. 9625087) and by the Wisconsin Groundwater Research Advisory Council (GRAC), which is administered through the University of Wisconsin System Water Resources Center. The findings and opinions

expressed herein are those of the authors and are not necessarily consistent with the policies and opinions of NSF or GRAC.

References

[1] D. Blowes, C. Ptacek, J. Cherry, R. Gillham, W. Robertson, Passive remediation of groundwater using in situ treatment curtains, geoenvironment 2000, ASCE GSP 46 (1995) 1588–1607.
[2] P.G. Tratnyek, T.L. Johnson, M.M. Scherer, G.R. Eykholt, Remediating groundwater with zero-valent metals: chemical considerations in barrier design, Ground Water Monitoring and Remediation 17 (4) (1997) 108–114.
[3] G.R. Eykholt, T. Sivavec, Contaminant transport issues for reactive-permeable barriers, geoenvironment 2000, ASCE GSP 46 (1995) 1608–1621.
[4] S. Benner, D. Blowes, C. Ptacek, A Full-Scale Porous Reactive Wall for Prevention of Acid Mine Drainage, Ground Water Monitoring and Remediation, 1997, pp. 99–107.
[5] A. Gavaskar, N. Gupta, B. Sass, R. Janosy, D. O'Sullivan, Permeable Barriers for Groundwater Remediation, Battelle Press, Columbus, 1998, pp. 43–48.
[6] M.Th. van Genuchten, Analytical solutions for chemical transport with simultaneous adsorption, zero-order production and first-order decay, J. Hydrology 49 (1981) 213–233.
[7] G.R. Eykholt, Uncertainty-based scaling of iron reactive barriers, in situ remediation of the geoenvironment, ASCE GSP No. 71 (1997) 41–55.
[8] S. O'Hannesin, R. Gillham, Long-term performance of an in situ iron wall for remediation of VOCs, Ground Water 36 (1) (1998) 164–170.
[9] A.L. Roberts, L.A. Totten, W.A. Arnold, D.R. Burris, T.J. Campbell, Reductive elimination of chlorinated ethylenes by zero-valent metals, Environ. Sci. Technol. 30 (8) (1996) 2654–2659.
[10] T.L. Johnson, M.M. Scherer, P.G. Tratnyek, Kinetics of halogenated organic compound degradation by iron metal, Environ. Sci. Technol. 30 (8) (1996) 2634–2640.
[11] D.R. Burris, R.M. Allen-King, V.S. Manoranjan, T.J. Campbell, G.A. Loraine, B. Deng, Chlorinated ethene reduction by cast iron: sorption and mass transfer, J. Environ. Eng. 124 (10) (1998) 1012–1019.
[12] G.R. Eykholt, Analytical solution for networks of irreversible first-order reactions, Water Research, accepted for publication 4/10/98, 1998.
[13] L. Gelhar, Stochastic Subsurface Hydrogeology, Prentice-Hall, Englewood Cliffs, NJ, 1993.
[14] E. Webb, Simulation of braided channel and topology topography, Water Resources Research 31 (10) (1995) 2603–2611.
[15] P. Riemersma, J. Bahr, M. Anderson, A comparison of geologic and stochastic approaches to characterization of heterogeneity and their effects on simulation of pump and treat systems, uncertainty in the geologic environment: from theory to practice, ASCE GSP 58 (1996) 1003–1018.
[16] M. McDonald, A. Harbaugh, A Modular Three-Dimensional Finite-Difference Ground-Water Flow Model, Techniques of Water-Resource Investigations of the United States Geologic Survey, United States Government Printing Office, Washington, DC, 1988.
[17] C. Zheng, PATH3D 3.0: A Ground-Water Path and Travel-Time Simulator, S.S. Papadopulos and Assoc, 1991.
[18] E. Webb, M. Anderson, Simulation of preferential flow in three-dimensional, heterogeneous fields with realistic internal architecture, Water Resources Research 32 (3) (1996) 533–545.
[19] J. Aiken, A Three-Dimensional Characterization of a Course Glacial Outwash Deposit Used for Modeling Contaminant Movement, Masters thesis, Department of Geology, University of Wisconsin-Madison, 1993.
[20] E. Webb, Simulating the Spatial Heterogeneity of Sedimentological and Hydrological Characteristics for Braided Stream Deposits, PhD Dissertation, Department of Geology, University of Wisconsin-Madison, 1992.
[21] P. Riemersma, Geostatistical Characterization of Heterogeneity, Simulation of Advection, Transport, and Evaluation of Pump-and-Treat Systems in Braided Stream Deposits, PhD Dissertation, Department of Geology, University of Wisconsin-Madison, 1997.

[22] P. Jussell, F. Stauffer, T. Dracos, Transport modeling in heterogeneous aquifer: 1. Statistical description and numerical generation of gravel deposits, Water Resources Research 30 (6) (1994) 1803–1817.
[23] P. Jussell, F. Stauffer, T. Dracos, Transport modeling in heterogeneous aquifer: 2. Three-dimensional transport model and stochastic numerical tracer experiments, Water Resources Research 30 (6) (1994) 1819–1831.
[24] L. Liang, N. Lorte, J.D. Goodlaxen, J. Clausen, Q. Fernando, R. Muftikian, Byproduct formation during the reduction of TCE by zero-valence iron and palladized iron, Ground Water Monitoring and Remediation 17 (1) (1997) 122–127.
[25] T.J. Campbell, D.R. Burris, A.L. Roberts, J.R. Wells, Trichloroethylene and tetrachloroethylene reduction in a metallic iron–water–vapor batch system, Environ. Toxicol. Chem. 16 (4) (1997) 625–630.